

Supporting Information

Improved Specific Capacity and Cycle Stability of Organic Cocrystal Lithium-ion Batteries through Charge Transfer

*Xudong Fan^a, Huibo Zhang^a, Kang Li^a, Zhongxin Dong^a, Jie Huang^b, Feng Teng^a, Haibo Fan^a,
Hui Jiang^{*c}, Xuexia He^{*b}, Peng Hu^{*a}*

^aSchool of Physics, Northwest University, 710127, Xi'an, China

^bSchool of Materials Science and Engineering, Shaanxi Normal University, 710119, Xi'an, China

^cSchool of Materials Science and Engineering, Tianjin University, Tianjin 300072, P.R. China

Contents

Figure S1. CV curves at a scan rate of 0.1 mV s^{-1} of (a) pyrene-FA, (b) BAA-FA, (c) chrysene-FA and (d) perylene-FA.

Figure S2. Nyquist plots of (a) pyrene-FA, FA and pyrene, (b) BAA-FA, FA and BAA, (c) chrysene-FA, FA and chrysene, and (d) perylene-FA, FA and perylene.

Figure S3. Reversible capacities cycled at various rates of (a)-(d) pyrene-FA, BAA-FA, chrysene-FA and perylene-FA.

Figure S4. Cycling performance of at 1 A g^{-1} of (a) BAA-FA, (b) chrysene-FA and (c) perylene-FA.

Figure S5. SEM images of pyrene-FA (a) initial materials, (b) after 2000 cycles at 1 A g^{-1} .

Figure S6. Pseudocapacitive contribution rate of pyrene-FA at different scanning speeds.

Figure S7. (a) CV plots of FA at different voltage scanning rates, (b) the value of b (slope) at different peak currents in the CV of FA after linear fitting.

Figure S8. Pseudocapacitive contribution rate of FA at different scanning speeds.

Table S1. Comparison of battery performance among different cocrystals.

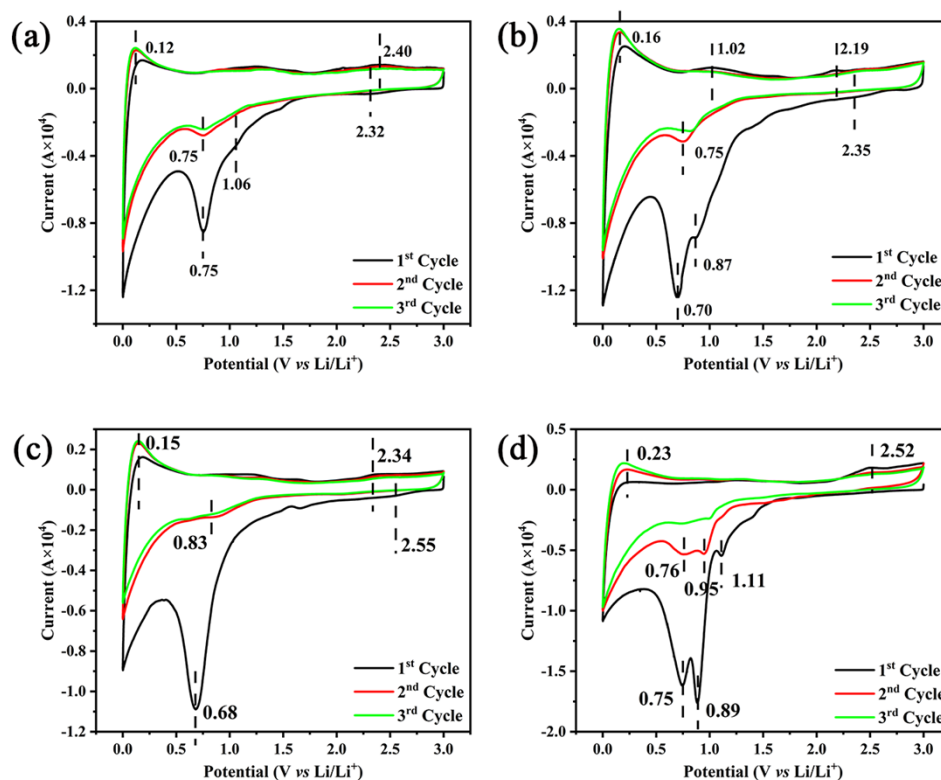


Figure S1. CV curves at a scan rate of 0.1 mV s^{-1} of (a) pyrene-FA, (b) BAA-FA, (c) chrysene-FA and (d) perylene-FA.

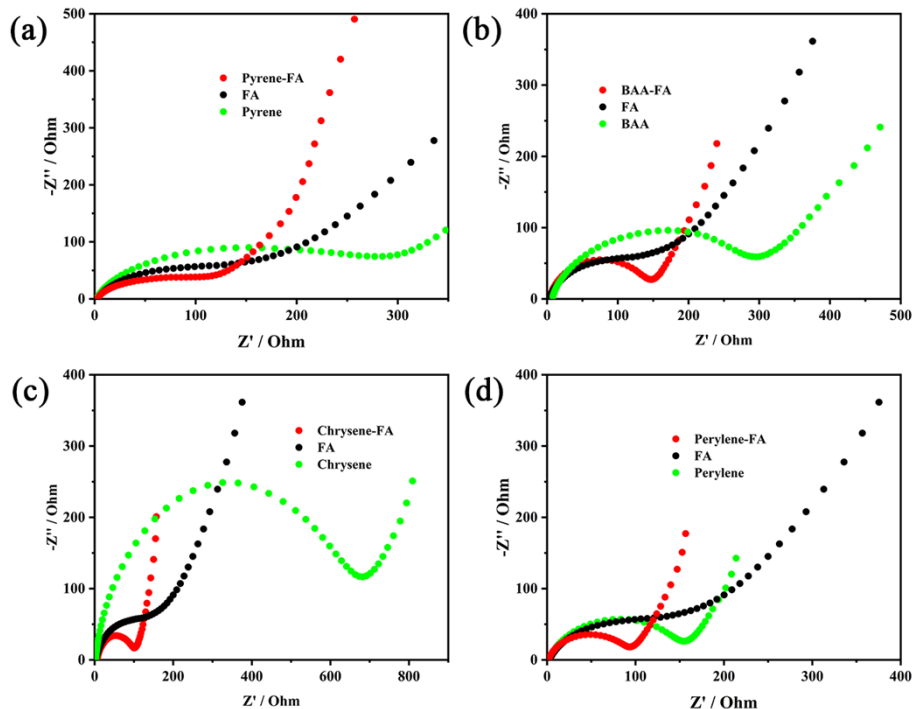


Figure S2. Nyquist plots of (a) pyrene-FA, FA and pyrene, (b) BAA-FA, FA and BAA, (c) chrysene-FA, FA and chrysene, and (d) perylene-FA, FA and perylene.

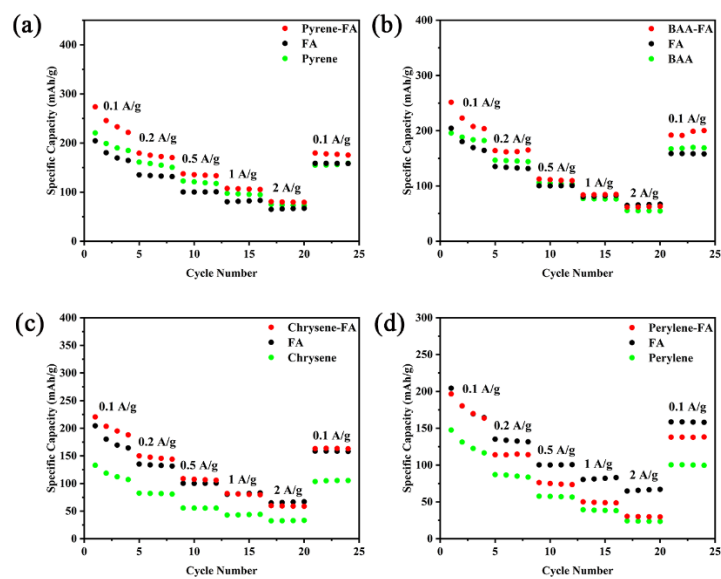


Figure S3. Reversible capacities cycled at various rates of (a)-(d) pyrene-FA, BAA-FA, chrysene-FA and perylene-FA.

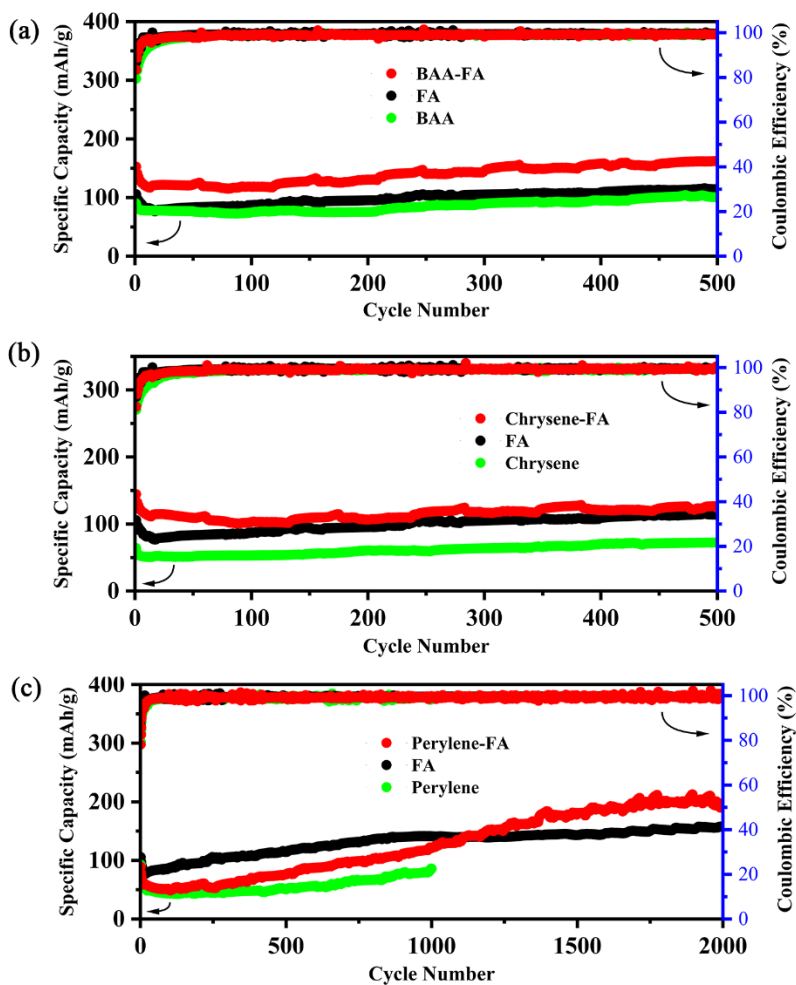


Figure S4. Cycling performance of at 1 A g⁻¹ of (a) BAA-FA, (b) chrysene-FA and (c) perylene-FA.

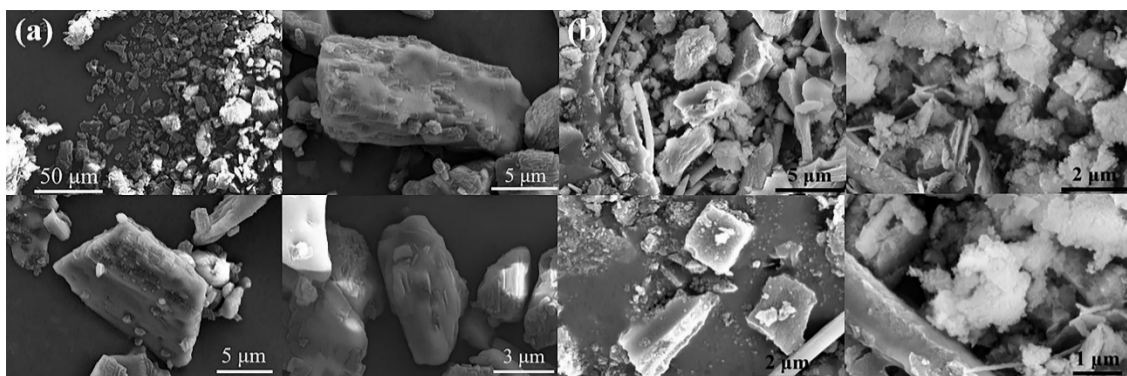


Figure S5. SEM images of pyrene-FA (a) initial materials, (b) after 2000 cycles at 1 A g⁻¹.

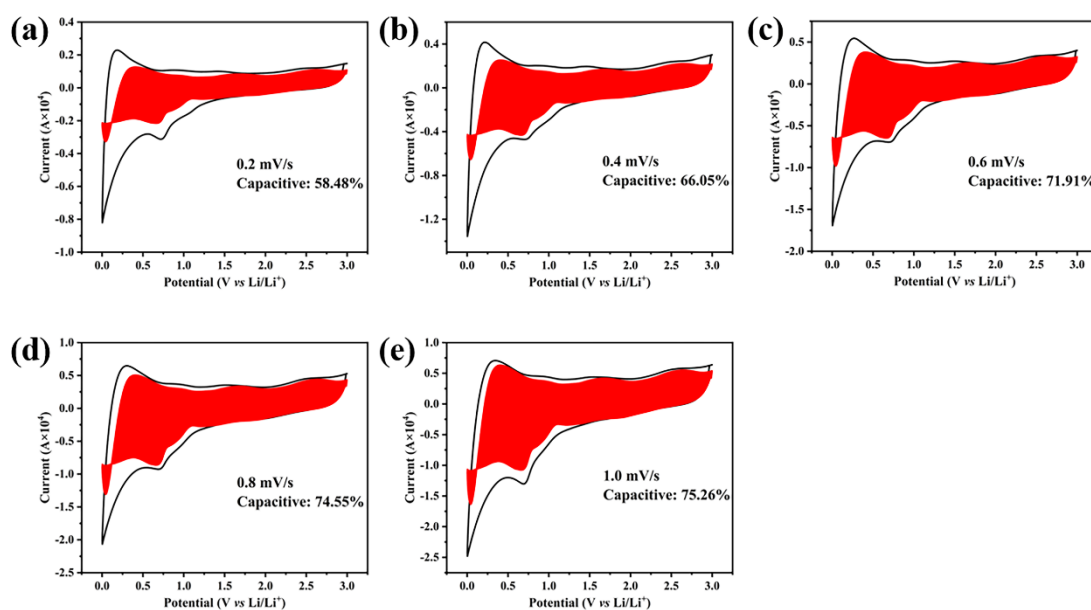


Figure S6. Pseudocapacitive contribution rate of pyrene-FA at different scanning speeds.

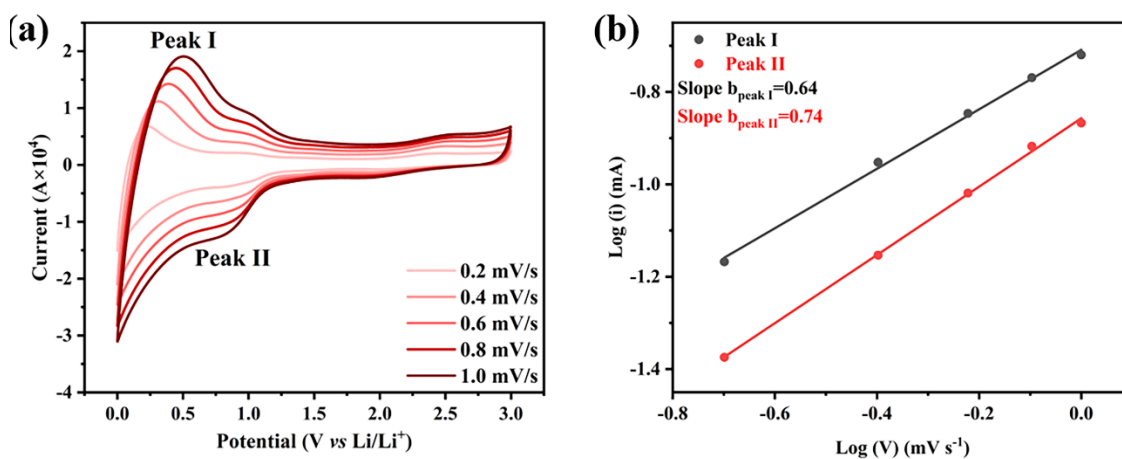


Figure S7. (a) CV plots of FA at different voltage scanning rates, (b) the value of b (slope) at different peak currents in the CV of FA after linear fitting.

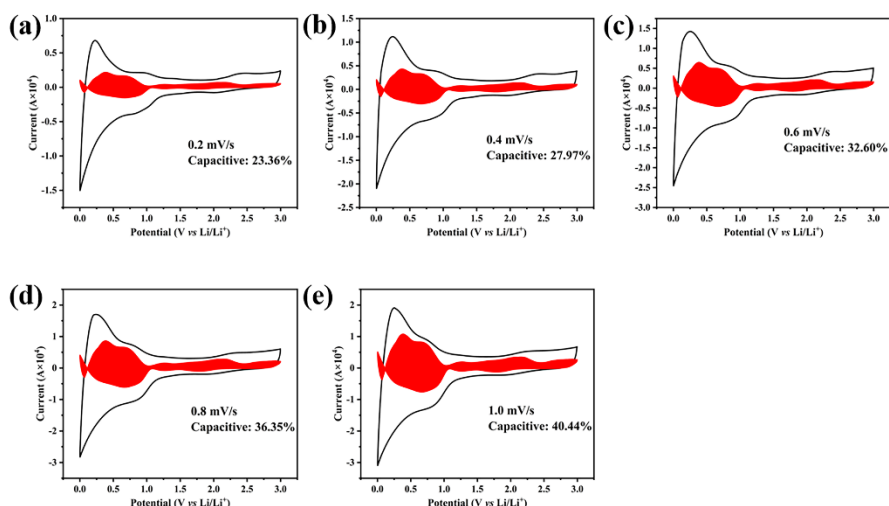


Figure S8. Pseudocapacitive contribution rate of FA at different scanning speeds.

Table S1. Comparison of battery performance among different cocrystals.

Cocrystal	Initial capacity	Cycling stability	Refs.
Coronene-HAT-CN	163.6 mAh g ⁻¹ at 0.1 A g ⁻¹	17.4% at 100 cycles	1
Pyrene-HAT-CN	28.7 mAh g ⁻¹ at 0.1 A g ⁻¹	35% at 100 cycles	1
Carbazole-HAT-CN	36.4 mAh g ⁻¹ at 0.1 A g ⁻¹	69% at 100 cycles	1
Corone-methyl-NDI	230 mAh g ⁻¹ at 0.5 A g ⁻¹	65% at 600 cycles	2
Corone-propyl-DNI	90 mAh g ⁻¹ at 0.5 A g ⁻¹	20% at 100 cycles	2
PNZ-TCNQ	98 mAh g ⁻¹ at 0.5 A g ⁻¹	73% at 50 cycles	3
DD-TCNQ	171 mAh g ⁻¹ at 0.05 A g ⁻¹	60% at 10 cycles	3
Li ₄ C ₈ H ₂ O ₆ -TCNQ	172 mAh g ⁻¹ at 0.5 C	58% at 100 cycles	4
Pyrene-FA	275 mAh g ⁻¹ at 0.1 A g ⁻¹	75% at 300 cycles	This work
Pyrene-FA	250 mAh g ⁻¹ at 1900 cycles	80% at 4500 cycles	This work

REFERENCES

1. K. Nakao, Y. Kamakura, M. Fujiwara, T. Shimizu, Y. Yoshida, H. Kitagawa, H. Yoshikawa, Y. Kitagawa and D. Tanaka, *Cryst. Growth Des.*, 2021, **22**, 26-31.
2. Z. Zheng, Z. Ju, S. Ma, Z. Liu, W. Xiang, J. Chen, B. Yang, Z. Mu, J. Zhang, P. Li and P. Sheng, *New J. Chem.*, 2023, **47**, 7476-7480.
3. S. Lee, J. Hong, S.-K. Jung, K. Ku, G. Kwon, W. M. Seong, H. Kim, G. Yoon, I. Kang, K. Hong, H. W. Jang and K. Kang, *Energy Storage Mater.*, 2019, **20**, 462-469.
4. F. Song, Z. Wang, T. Ma, L. Chen, H. Li and F. Wu, *Nano Energy*, 2023, **117**, 108893.